Extended surface disorder in the quantum Ising chain

1999 J. Phys. A: Math. Gen. 32 3907

(http://iopscience.iop.org/0305-4470/32/21/304)

J. Phys. A: Math. Gen. **32** (1999) 3907–3918. Printed in the UK PII: S0305-4470(99)02262-3

Extended surface disorder in the quantum Ising chain

L Turban†, D Karevski† and F Iglói‡

† Laboratoire de Physique des Matériaux, Université Henri Poincaré (Nancy I), BP 239, F–54506 Vandœuvre lès Nancy Cedex, France

‡ Research Institute for Solid State Physics and Optics, PO Box 49, H–1525 Budapest, Hungary and Institute of Theoretical Physics, Szeged University, H–6720 Szeged, Hungary

Received 3 March 1999

Abstract. We consider random extended surface perturbations in the transverse field Ising model decaying as a power of the distance from the surface towards a pure bulk system. The decay may be linked either to the evolution of the couplings or to their probabilities. Using scaling arguments, we develop a relevance–irrelevance criterion for such perturbations. We study the probability distribution of the surface magnetization, its average and typical critical behaviour for marginal and relevant perturbations. According to analytical results, the surface magnetization follows a log-normal distribution and both the average and typical critical behaviours are characterized by power-law singularities with continuously varying exponents in the marginal case and essential singularities in the relevant case. For enhanced average local couplings, the transition becomes first order with a nonvanishing critical surface magnetization. This occurs above a positive threshold value of the perturbation amplitude in the marginal case.

1. Introduction

Quenched, i.e., time-independent disorder has a strong influence on the nature of quantum phase transitions which take place at zero temperature [1]. Many interesting features of the effect of randomness can be observed in one-dimensional systems for which several exact results have been obtained. Recently, the one-dimensional random transverse-field Ising model (TIM) has been the subject of much interest. It is defined by the Hamiltonian

$$\mathcal{H} = -\tfrac{1}{2}\sum_l (J_l \sigma_l^z \sigma_{l+1}^z + h_l \sigma_l^x) \tag{1.1}$$

where σ_l^x and σ_l^z are Pauli matrices at site l and the exchange couplings, J_l, the transverse fields, h_l, are random variables.

For homogeneous independently distributed couplings and fields, Fisher [2, 3] obtained many new results about the static properties of the random TIM in (1.1) using a real space renormalization group method which is believed to become exact at large scales, i.e., sufficiently close to the critical point. Later, Fisher's conjectures have been checked numerically [4–6] and new results have been obtained, especially about the dynamical properties of the model at the critical point [7, 8] as well as in the Griffiths phase [9, 10].

In many physical situation the disorder is not homogeneous. A free surface or a defect in the bulk can evidently induce a disorder which is inhomogeneously distributed in its vicinity. In this paper we consider a random version of the Hilhorst–van Leeuwen (HvL) model [11–13]. In this model, the couplings are modified near a free surface and the amplitude of the perturbation

0305-4470/99/213907+12$19.50

decays according to a power law $l^{-\kappa}$ where l denotes the distance from the surface. A relevance–irrelevance criterion has been proposed for such smoothly inhomogeneous perturbations, showing that marginal behaviour is obtained when the decay exponent $\kappa = 1/\nu$ where ν is the correlation length exponent of the pure system [14–16]. The critical behaviour is then characterized by local exponents which vary continuously with the perturbation amplitude. For a slower decay the perturbation becomes relevant and, locally, power laws are replaced by essential singularities.

We consider two types of random extended surface perturbations associated with a pure bulk system.

For the first type of perturbation, the probabilities p_l and q_l are constant and the couplings take the values:

$$J_l = J\left[1 + a_1\frac{(-1)^{f_l}}{l^\kappa}\right] \qquad f_l = \begin{cases} 1 & p_l = \frac{1}{2} \\ 0 & q_l = \frac{1}{2} \end{cases} \qquad \text{(model \#1).} \quad (1.2)$$

The perturbation has a vanishing average and the couplings decay towards their constant bulk value J.

For the second type, the decay is associated with the probabilities whereas the amplitudes remain constant. The couplings follow the binary distribution:

$$J_l = J(1 + f_l a_2) \qquad f_l = \begin{cases} 1 & p_l = l^{-\kappa} \\ 0 & q_l = 1 - l^{-\kappa} \end{cases} \qquad \text{(model \#2).} \quad (1.3)$$

The average coupling takes the same form as in the HvL model and one recovers asymptotically a pure bulk system with couplings equal to J.

The transverse field is always assumed to be constant, $h_l = h = 1$, thus the bulk is critical at $J = 1$.

In this paper, we study the surface magnetic properties in the marginal situation which occurs at $\kappa = \frac{1}{2}$ for model #1 and $\kappa = 1$ for model #2 as well as for relevant perturbations corresponding to slower decays.

The same type of problem with an aperiodic distribution of the couplings following some substitution sequence has been considered recently [17].

The structure of the paper is the following. The relevance of random extended surface perturbations is discussed in section 2. In section 3, analytical results about the surface magnetization of the inhomogeneous TIM are presented. The two models of inhomogeneous surface disorder are studied in section 4 for marginal perturbations and section 5 for relevant ones. The results are discussed in section 6.

2. Relevance–irrelevance criterion

We begin with a discussion of the relevance of random extended surface perturbations in a d-dimensional classical system. The unperturbed system has a free surface of dimension $d-1$ at $l = 0$, perpendicular to the unit vector $\boldsymbol{u}$, and the position vector is written as $\boldsymbol{r} = l\boldsymbol{u} + \boldsymbol{r}_\parallel$. The layered perturbation, which couples to the operator density $\phi(\boldsymbol{r})$ with bulk scaling dimension x_ϕ, is written as

$$-\beta V = \sum_{\boldsymbol{r}} A(l)\phi(\boldsymbol{r}) \quad (2.1)$$

where $\beta = (k_B T)^{-1}$. The perturbation amplitude $A(l)$ in the different layers are independent random variables such that:

$$\begin{aligned} &[A(l)]_{\rm av} = 0 \qquad [A(l)A(l')]_{\rm av} = \frac{A_1^2}{l^{2\kappa}}\delta_{ll'} \qquad \text{(model \#1)} \\ &[A(l)]_{\rm av} = \frac{A_2}{l^{\kappa}} \qquad [A(l)A(l')]_{\rm av} = \frac{A_2^2}{l^{\kappa}}\delta_{ll'} + \frac{A_2^2}{(ll')^{\kappa}}(1-\delta_{ll'}) \qquad \text{(model \#2).} \end{aligned} \tag{2.2}$$

Thermodynamic perturbation theory, up to second order, gives the following correction to the free energy:

$$\begin{aligned} -\beta\Delta F &= -\beta\langle V\rangle + \tfrac{1}{2}\beta^2[\langle V^2\rangle - \langle V\rangle^2] \\ &= \sum_{\boldsymbol{r}} A(l)\langle\phi(\boldsymbol{r})\rangle + \tfrac{1}{2}\sum_{\boldsymbol{r},\boldsymbol{r}'} A(l)A(l')\mathcal{G}_{\phi\phi}(\boldsymbol{r},\boldsymbol{r}') \end{aligned} \tag{2.3}$$

where $\langle\cdots\rangle$ denotes a thermal average and $\mathcal{G}_{\phi\phi}$ is the connected two-point correlation function of the operator $\phi(\boldsymbol{r})$, both for the unperturbed system.

In the case of model #1, the average of the first-order correction vanishes. The relevance of the perturbation is linked to the scaling behaviour of the amplitude in the average of the second-order correction

$$-\beta[\Delta F^{(2)}]_{\rm av} = \frac{L^{d-1}}{2}\sum_{l}\sum_{\boldsymbol{r}_\parallel}\frac{A_1^2}{l^{2\kappa}}\mathcal{G}_{\phi\phi}(r_\parallel) \tag{2.4}$$

where L^{d-1} is the surface of the layers. The average perturbation density has dimension $2d-1$ wheras the correlation function has dimension $2x_\phi$, thus, under a length rescaling by a factor $b = L/L'$,

$$\frac{A_1'^2}{l'^{2\kappa}} = b^{2d-1-2x_\phi}\frac{A_1^2}{l^{2\kappa}} = b^{2y_\phi-1}\frac{A_1^2}{l^{2\kappa}} \tag{2.5}$$

and the second-order perturbation amplitude transforms as

$$A_1'^2 = b^{2y_\phi-2\kappa-1}A_1^2 \tag{2.6}$$

where $y_\phi = d - x_\phi$ is the bulk scaling dimension of the variable conjugate to ϕ. It follows that the perturbation is marginal when $\kappa = \kappa_1 = y_\phi - \frac{1}{2}$. It becomes relevant (irrelevant) when $\kappa < (>)\kappa_1$.

In the case of model #2, the average of the first-order correction is given by

$$-\beta[\Delta F^{(1)}]_{\rm av} = \sum_{\boldsymbol{r}}\frac{A_2}{l^{\kappa}}\langle\phi(\boldsymbol{r})\rangle. \tag{2.7}$$

The average perturbation density has now dimension d so that

$$\frac{A'_2}{l'^{\kappa}} = b^{d-x_\phi}\frac{A_2}{l^{\kappa}} = b^{y_\phi}\frac{A_2}{l^{\kappa}} \tag{2.8}$$

and

$$A'_2 = b^{y_\phi-\kappa}A_2. \tag{2.9}$$

The perturbation is marginal when $\kappa = \kappa_2 = y_\phi$, relevant (irrelevant) when $\kappa < (>)\kappa_2$. One may notice that the average perturbation is of the HvL form, thus the relevance criterion is the same for both models to first order in the perturbation amplitude. A scaling analysis of the second-order correction contributed by the off-diagonal term in $[A(l)A(l')]_{\rm av}$ leads to the same conclusion. Comparing the form of $[A(l)A(l')]_{\rm av}$ for both models, one concludes that the

diagonal second-order correction in model #2 scales as A_1^2 in equation (2.6) with 2κ replaced by κ, i.e., as

$$[A'^2_2]_{\text{diag}} = b^{2y_\phi-\kappa-1}[A_2^2]_{\text{diag}}. \tag{2.10}$$

It follows that the second-order diagonal correction is relevant when $\kappa < 2y_\phi - 1$. It is more dangerous than the first-order correction when $y_\phi > 1$.

In the case of the two-dimensional Ising model with a thermal perturbation, such that $\phi(\boldsymbol{r})$ is the energy density $\sigma_{\boldsymbol{r}}\sigma_{\boldsymbol{r}+\boldsymbol{u}}$, one has $y_\phi = 1/\nu = 1$ and marginal behaviour is obtained for $\kappa_1 = \frac{1}{2}$ and $\kappa_2 = 1$ as indicated in the introduction.

The one-dimensional TIM, defined in equation (1.1) together with (1.2) or (1.3), which corresponds to the extreme anisotropic limit of the two-dimensional classical systems discussed here [18], belongs to the same universality class, i.e., the relevance of the perturbation is the same for both problems.

3. Surface magnetization and surface correlations

Let us consider the imaginary time spin–spin autocorrelation function of the TIM

$$\mathcal{G}_l(\tau) = \langle 0|\sigma_l^z(\tau)\sigma_l^z(0)|0\rangle = \sum_i |\langle i|\sigma_l^z|0\rangle|^2 \exp[-\tau(E_i - E_0)] \tag{3.1}$$

where $|0\rangle$ and $|i\rangle$ denotes the ground state and the ith excited state of $\mathcal{H}$ in equation (1.1), with energies E_0 and E_i, respectively. With symmetry-breaking boundary conditions, i.e., fixing the spin at the other end of the chain, such that $\sigma_L^z = \pm 1$, the ground state of the system is degenerate and in the large-τ limit we have $\lim_{\tau\to\infty}\mathcal{G}_l(\tau) = m_l^2$, with a local magnetization given by

$$m_l = \langle 1|\sigma_l^z|0\rangle. \tag{3.2}$$

To calculate m_l we use the standard methods of Lieb, Schultz and Mattis [19] and transform $\mathcal{H}$ into a free-fermion Hamiltonian,

$$\mathcal{H} = \sum_{q=1}^{L} \epsilon_q(\eta_q^\dagger\eta_q - \tfrac{1}{2}) \tag{3.3}$$

in terms of the fermion creation (annihilation) operators $\eta_q^\dagger$ (η_q). On a chain with length L and free boundary conditions, the non-negative fermion excitations ϵ_q satisfy the set of equations

$$\begin{aligned} \epsilon_q\psi_q(l) &= -h_l\varphi_q(l) - J_l\varphi_q(l+1) \\ \epsilon_q\varphi_q(l) &= -J_{l-1}\psi_q(l-1) - h_l\psi_q(l) \end{aligned} \tag{3.4}$$

with $J_0 = J_L = 0$. Introducing the $2L$-dimensional vector $\boldsymbol{V}_q$ with components

$$V_q(2l-1) = -\varphi_q(l) \qquad V_q(2l) = \psi_q(l) \tag{3.5}$$

the relations in equation (3.4) lead to an eigenvalue problem for the tridiagonal matrix

$$\mathsf{T} = \begin{pmatrix} 0 & h_1 & & & & \\ h_1 & 0 & J_1 & & & \\ & J_1 & 0 & h_2 & & \\ & & \ddots & \ddots & \ddots & \\ & & & J_{L-1} & \ddots & h_L \\ & & & & h_L & 0 \end{pmatrix}. \tag{3.6}$$

Taking the square of T, odd and even components of $\boldsymbol{V}_q$ decouple and one recovers two separate eigenvalue problems for φ and ψ. According to equation (3.4), changing φ_q into $-\varphi_q$ in $\boldsymbol{V}_q$,

the eigenvector corresponding to $-\epsilon_q$ is obtained. Thus all the needed information is contained in that part of the spectrum of $\mathbf{T}$ with $\epsilon_q \geqslant 0$. Later on we shall restrict ourselves to this sector.

Fixing the surface spin at $l = L$ amounts to putting $h_L = 0$ in $\mathbf{T}$, thus the lowest excitation $\epsilon_1 = 0$ and the ground state of the system is degenerate.

Using Wick's theorem, one may show that the local magnetization m_l, with a fixed spin at $l = L$, is given by a determinant [8]. For the surface spin, at $l = 1$, the expression simplifies considerably and the surface magnetization takes the form [20]:

$$m_s(L) = m_1 = \varphi_1(1) = \left[1 + \sum_{l=1}^{L-1} \prod_{k=1}^{l} \left(\frac{h_k}{J_k}\right)^2\right]^{-\frac{1}{2}}. \tag{3.7}$$

This can be rewritten under the equivalent form

$$m_s(L) = \overline{m}_s^d(L) \prod_{l=1}^{L-1} \left(\frac{J_l}{h_l}\right) \tag{3.8}$$

where $\overline{m}_s^d$ is the surface magnetization at $l = L$ for the dual chain (for which the fields and the couplings are exchanged, $h_l \leftrightarrow J_l$) with a fixed spin now at $l = 1$.

We shall illustrate the usefulness of the last expression on the example of the HvL model which corresponds to the Hamiltonian (1.1) with $h_l = 1$ and $J_l = J(1 + al^{-\kappa})$. In the marginal situation, $\kappa = 1$, the product in (3.8) asymptotically behaves as $\prod_{l=1}^{L} J_l \sim L^a$ at the critical point, $J_c = 1$. Furthermore, when $L \gg 1$, the couplings at the other end of the chain are asymptotically unperturbed, thus one expects that $\overline{m}_s^d(L) \sim L^{-\frac{1}{2}}$, as for the homogeneous model at the ordinary transition. Then from (3.8) we deduce the continuously varying dimension

$$x_m^s = \tfrac{1}{2} - a \qquad a \leqslant \tfrac{1}{2} \tag{3.9}$$

which governs the scaling behaviour of the surface magnetization, $m_s(L) \sim L^{-x_m^s}$. This expression is valid only for $a \leqslant \frac{1}{2}$ since x_m^s must be non-negative. When $a > a_c = \frac{1}{2}$, $x_m^s = 0$, i.e., the critical surface magnetization remains finite for the semi-infinite system. It follows that our assumption about the scaling behaviour of $\overline{m}_s^d$ should be corrected in the regime of first-order transition ($a > \frac{1}{2}$). It has to compensate the contribution of the product in (3.8), thus $\overline{m}_s^d \sim L^{-a}$. Since we are considering the magnetization of the dual chain, with couplings $J_l^d(a) = 1/J_l(a) \simeq J_l(-a)$, this means that when the couplings are sufficiently weak ($a < -\frac{1}{2}$) near $l = 1$, the finite-size-scaling behaviour of the critical magnetization at $l = L$ is anomalous.

When the perturbation is relevant, $\kappa < 1$, the product of the couplings leads to a stretched exponential behaviour,

$$m_s \sim \exp\left(\frac{a}{1-\kappa} L^{1-\kappa}\right) \tag{3.10}$$

which is clearly valid only when $a < 0$. Otherwise the dual magnetization term contributes, giving a size-independent result which corresponds to an ordered surface when $a > 0$ [20].

4. Marginal extended surface disorder

In this section we consider marginal random extended perturbations at the surface of the TIM. The transverse field is uniform, $h_l = h = 1$, and the distributions of the couplings J_l are given by either (1.2) with $\kappa = \frac{1}{2}$ or (1.3) with $\kappa = 1$ for marginal behaviour.

The finite-size-scaling behaviour of the *average* critical surface magnetization at $J = 1$ is deduced for both models from equation (3.8) for $L \gg 1$. As for the HvL model, one expects

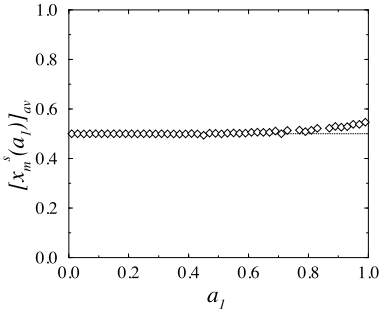

Figure 1. Scaling dimension of the average surface magnetization as a function of the perturbation amplitude for model #1. The dotted line corresponds to the analytical result in equation (4.1).

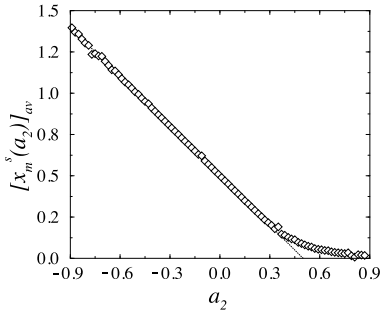

Figure 2. Scaling dimension of the average surface magnetization as a function of the perturbation amplitude for model #2. The dotted line corresponds to the analytical result in equation (4.1).

$\overline{m}_s^d$ on the unperturbed end to scale as $L^{-\frac{1}{2}}$, as long as the transition is continuous, while the average of the product behaves as $[\prod_{l=1}^{L} J_l]_{av} = \prod_{l=1}^{L}[J_l]_{av}$.

For model #1, $[J_l]_{av} = J = 1$ and $[m_s]_{av} \sim L^{-\frac{1}{2}}$, whereas $\prod_{l=1}^{L}[J_l]_{av} \sim L^{a_2}$ for model #2. Thus we obtain the following values for the scaling dimension of the average surface magnetization:

$$[x_m^s]_{av} = \tfrac{1}{2} \quad \text{(model \#1)} \qquad \begin{cases} [x_m^s]_{av} = \frac{1}{2} - a_2 & a_2 \leqslant \frac{1}{2} \\ [x_m^s]_{av} = 0 & a_2 > \frac{1}{2} \end{cases} \quad \text{(model \#2).} \tag{4.1}$$

As for the HvL model there is a finite average surface magnetization at the critical point for strong enough local couplings, i.e., for $a_2 > \frac{1}{2}$ where $\lim_{L\to\infty}[m_s]_{av} > 0$. In this first-order regime the dual magnetization no longer scales as $L^{-1/2}$. Actually, the correlation between the two factors on the rhs of equation (3.8) modifies the scaling behaviour of the average of the product, leading to $[x_m^s]_{av} = 0$. One may notice that since the bulk Ising system has a correlation length exponent $\nu = 1$, equation (4.1) also gives the surface magnetic exponent $[\beta_s]_{av} = [x_m^s]_{av}$.

The results for the average surface magnetization have been checked numerically, considering 10^6 realizations of randomly inhomogeneous quantum spin chains and computing the critical magnetization $m_s(L)$ given by (3.7) for chain sizes $L = 2^5$ to 2^{14}. The exponents were deduced from an extrapolation of two-point approximants using the BST algorithm [21]. The variations of the average surface magnetic exponents, shown in figures 1 and 2, are in excellent agreement with the expected ones.

Next we are going to study the probability distribution of the surface magnetization for the two models. Again we start from equation (3.8) in which, for large L, $\overline{m}_s^d$, which refers to the unperturbed end, is expected to scale as $L^{-\frac{1}{2}}$ as long as the transition on the other surface is second order. Thus, in the second-order regime, the central limit theorem can be applied to the random variable $\ln m_s + \frac{1}{2}\ln L = \sum_{l=1}^{L}\ln(J_l)$ and $\ln m_s$ follows a normal distribution

$$P_L(\ln m_s) \simeq \frac{1}{\sqrt{2\pi\,\mathrm{var}(\ln m_s)}} \exp\left[-\frac{(\ln m_s - [\ln m_s]_{av})^2}{2\mathrm{var}(\ln m_s)}\right] \tag{4.2}$$

where $\mathrm{var}(\ln m_s) = [(\ln m_s - [\ln m_s]_{av})^2]_{av}$. This expression is valid for $L \gg 1$ and $\ln m_s \ll 0$. It does not correctly describe the rare events, governing the average behaviour, which correspond to the tail of the distribution near $\ln m_s = 0$.

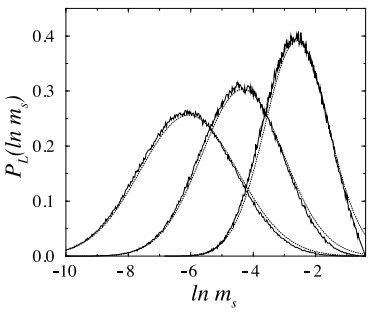

Figure 3. Probability distribution of $\ln m_s$ calculated on 10^6 samples for model #1. The perturbation amplitude is $a_1 = 0.5$ and the chain sizes are $L = 2^6$, 2^{10} and 2^{14} from right to left. The dotted curve corresponds to the normal distribution in equation (4.2).

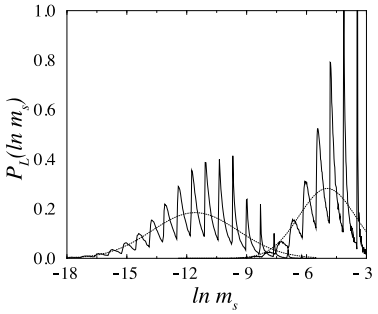

Figure 4. Probability distribution of $\ln m_s$ calculated on 10^6 samples for model #2 in the second-order regime. The perturbation amplitude is $a_2 = -0.5$ and the chain sizes are $L = 2^6$ and 2^{14} from right to left. The dotted curve corresponds to the normal distribution in equation (4.2). The actual distribution displays strong periodic oscillations around the normal distribution.

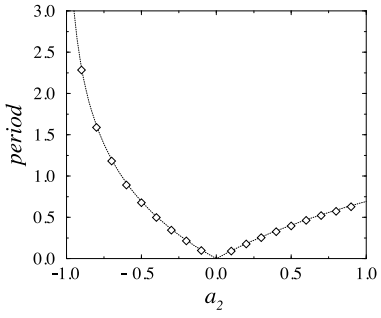

Figure 5. Variation of the period of oscillations in the distribution $P_L(\ln m_s)$ for model #2 as a function of the marginal amplitude a_2. The points give the periods deduced from the numerical data for the largest size, $L = 2^{14}$, and the dotted curve corresponds to $|\ln(1+a_2)|$.

The parameters of the distribution are easily deduced from equations (1.2) and (1.3) and read:

$$\left.\begin{aligned} &[\ln m_s]_{\rm av} \simeq -\frac{1}{2}\ln L - \sum_{l=1}^{L}\frac{a_1^2}{2l} \simeq -\frac{1}{2}(1+a_1^2)\ln L \\ &{\rm var}(\ln m_s) \simeq a_1^2 \ln L \end{aligned}\right\} \quad \text{(model \#1)}$$

$$\left.\begin{aligned} &[\ln m_s]_{\rm av} \simeq -\frac{1}{2}\ln L + \sum_{l=1}^{L}\frac{\ln(1+a_2)}{l} \simeq -\left[\frac{1}{2} - \ln(1+a_2)\right]\ln L \\ &{\rm var}(\ln m_s) \simeq \ln^2(1+a_2)\ln L \end{aligned}\right\} \quad \text{(model \#2).} \tag{4.3}$$

The distributions $P_L(\ln m_s)$, obtained through numerical calculations on 10^6 samples for different chain sizes, are compared with the analytical expressions in figures 3 and 4. The agreement is quite good at large sizes, although the normal distribution is strongly modulated for model #2. As shown in figure 5, the modulation involves a periodic function of period 1 in the variable $\ln m_s/|\ln(1+a_2)|$, where $1+a_2$ is the ratio of the two couplings in equation (1.3). The oscillations are log-periodic in the variable m_s (see [22] for a recent review about log-periodic phenomena).

The probability distribution is centred on $[\ln m_s]_{\rm av} = \ln[m_s]_{\rm typ} \sim \ln L$, where $[m_s]_{\rm typ}$ is the most probable or *typical* value of the surface magnetization. Consequently, the typical magnetization scales as a power of L, $[m_s]_{\rm typ} \sim L^{-[x_m^s]_{\rm typ}}$, with a continuously varying typical

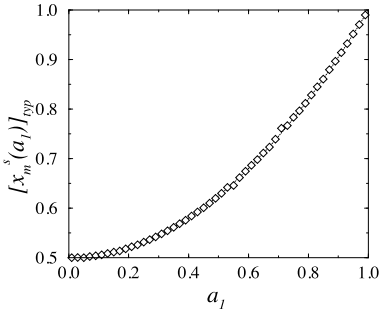

Figure 6. Scaling dimension of the typical surface magnetization as a function of the perturbation amplitude a_1 for model #1. The dotted curve corresponds to the analytical result in equation (4.4).

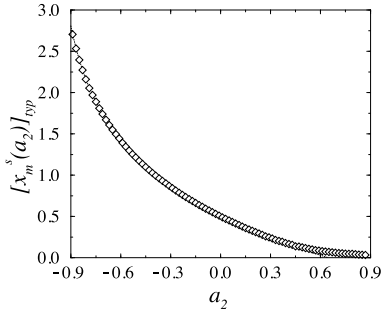

Figure 7. Scaling dimension of the typical surface magnetization as a function of the perturbation amplitude for model #2. The dotted curve corresponds to the analytical result in equation (4.4).

exponent given by:

$$\left.\begin{array}{ll} [x_{\rm m}^{\rm s}]_{\rm typ} = \frac{1}{2}(1+a_1^2) & \\ [x_{\rm m}^{\rm s}]_{\rm typ} = \frac{1}{2} - \ln(1+a_2) \qquad a_2 \leqslant \sqrt{\rm e} - 1 & \\ [x_{\rm m}^{\rm s}]_{\rm typ} = 0 \qquad a_2 > \sqrt{\rm e} - 1 & \end{array}\right\} \quad \begin{array}{l} \text{(model \#1)} \\ \\ \text{(model \#2).} \end{array} \tag{4.4}$$

In model #1, the typical surface magnetization vanishes continuously at the bulk critical point for any value of the perturbation amplitude. In model #2, for strong enough local couplings, $a_2 > [a_{2c}]_{\rm typ} = \sqrt{\rm e} - 1 \simeq 0.6487$, there is a first-order surface transition, the typical surface magnetization remaining nonvanishing at criticality. In the range $\frac{1}{2} < a_2 < \sqrt{\rm e} - 1$, at the bulk critical point, $[m_{\rm s}]_{\rm av} > 0$ whereas $[m_{\rm s}]_{\rm typ} = 0$ when $L \to \infty$, a behaviour which is consistent with the fact that $[\ln m_{\rm s}]_{\rm av} \leqslant \ln[m_{\rm s}]_{\rm av}$.

The numerical results for the scaling dimension of the typical surface magnetization are shown in figures 6 and 7. Two-point finite-size approximants were extrapolated using the BST algorithm and we used the same samples as for the average magnetization. The agreement with the expressions given in (4.4) is quite good.

5. Relevant extended surface disorder

Let us now examine the modified surface critical behaviour induced by relevant extended surface disorder which, according to the disussion of section 2, corresponds to a decay exponent κ in equations (1.2) and (1.3) lower than $\kappa_1 = \frac{1}{2}$ for model #1 and $\kappa_2 = 1$ for model #2, respectively.

Like in the marginal case, the average surface magnetization obtained by averaging equation (3.8) would scale with an exponent $[x_{\rm m}^{\rm s}]_{\rm av} = \frac{1}{2}$ for model #1 if the dual magnetization was unaffected by the perturbation. A numerical finite-size scaling study with $a_1 = 0.5$ and $\kappa = 0.25$, shows that the actual behaviour is a stretched exponential one since $\ln[m_{\rm s}]_{\rm av} \sim L^{1/2}$, as shown in figure 8. Thus the slowly decaying perturbation changes the critical behaviour on the second surface. By symmetry, the behaviour is the same for negative values of a_1. Numerical studies for other values of κ indicate that the argument of the stretched exponential involves the power $L^{1-2\kappa}$.

For model #2, taking only into account the product of the couplings, one obtains

$$[m_{\rm s}]_{\rm av} \sim \exp\left[\frac{a_2}{1-\kappa} L^{1-\kappa}\right]. \tag{5.1}$$

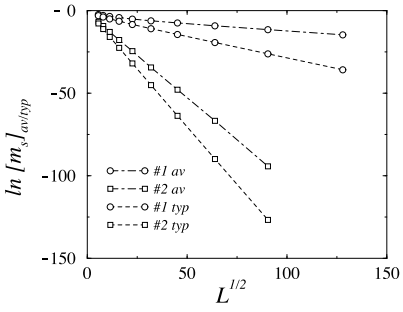

Figure 8. Finite-size scaling of the average (dot-dashed lines) and typical (dashed lines) surface magnetization with relevant perturbations illustrating the stretched exponential behaviour. The parameters are $a_1 = 0.5$ and $\kappa = 0.25$ for model #1 (circles), $a_2 = -0.5$ and $\kappa = 0.5$ for model #2 (squares). Averages were taken over 10^6 samples.

Hence the average surface magnetization has a stretched exponential dependence on L for negative values of the amplitude a_2. The numerical data are in agreement with this behaviour as shown in figure 8 for $a_2 = -0.5$ and $\kappa = 0.5$. The value of the slope, -0.99 ± 0.04, is close to the analytical result, -1. Thus the dual magnetization is likely to contribute here only through a power of L in front of the exponential.

When $a_2 > 0$, the divergence of $[m_s]_{av}$ with the system size signals that the dual magnetization term in (3.8) can no longer be neglected. The surface transition is then first order. This was checked numerically at $a_2 = 0.5$ where the average critical surface magnetization is indeed size-independent at large L values. Contrary to the case of a marginal perturbation where a mininum enhancement of the couplings was needed to maintain surface order at the bulk critical point, here a first-order surface transition occurs for any positive value of the perturbation amplitude. The same behaviour is obtained with the HvL model [20].

The probability distribution $P_L(\ln m_s)$ can be obtained in the same way as in the marginal situation when the transition is continuous, provided that $\ln m_s$ is dominated by the contribution of the product in (3.8). Then one recovers the normal distribution of equation (4.2) with the following parameters:

$$\left.\begin{aligned} [\ln m_s]_{av} &\simeq -\sum_{l=1}^{L} \frac{a_1^2}{2l^{2\kappa}} \simeq -\frac{a_1^2}{2(1-2\kappa)} L^{1-2\kappa} \\ \mathrm{var}(\ln m_s) &\simeq \tfrac{a_1^2}{1-2\kappa} L^{1-2\kappa} \end{aligned}\right\} \quad \text{(model \#1)}$$

$$\left.\begin{aligned} [\ln m_s]_{av} &\simeq \sum_{l=1}^{L} \frac{\ln(1+a_2)}{l^{\kappa}} \simeq \frac{\ln(1+a_2)}{1-\kappa} L^{1-\kappa} \\ \mathrm{var}(\ln m_s) &\simeq \tfrac{\ln^2(1+a_2)}{1-\kappa} L^{1-\kappa} \end{aligned}\right\} \quad \text{(model \#2).} \tag{5.2}$$

The numerical data, shown in figures 9 and 10, were deduced from 10^5 realizations and, as above, with $a_1 = 0.5$, $\kappa = 0.25$ for model #1 and $a_2 = -0.5$, $\kappa = 0.5$ for model #2.

In the case of model #1, the shift with respect to the analytical results confirms a weak relevant contribution of the dual magnetization term in (3.8). This is confirmed in figure 8 where the slope of $\ln[m_s]_{typ}$ versus $L^{1-2\kappa}$ is 0.266 ± 0.003 to be compared with the value -0.25 given by (5.2).

The agreement is much better for model #2. Here the slope of $\ln[m_s]_{typ}$ versus $L^{1-\kappa}$ in figure 8, -1.401 ± 0.002, has a smaller relative deviation from the expected value, -1.386. One may notice that the probability distribution no longer displays the strong log-periodic modulations observed in the marginal case.

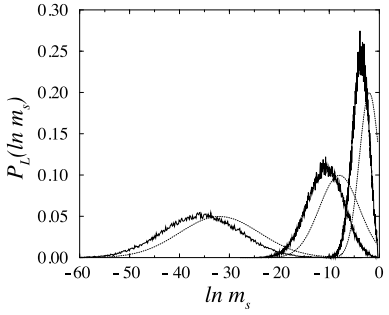

Figure 9. Probability distribution of $\ln m_s$ calculated on 10^5 samples for model #1 with a relevant perturbation. The amplitude is $a_1 = 0.5$ and the decay exponent $\kappa = 0.25$. The chain sizes are $L = 2^6$, 2^{10} and 2^{14} from right to left. The dotted curves correspond to the normal distribution in equation (4.2) when the contribution of the dual magnetization to $\ln m_s$ is neglected.

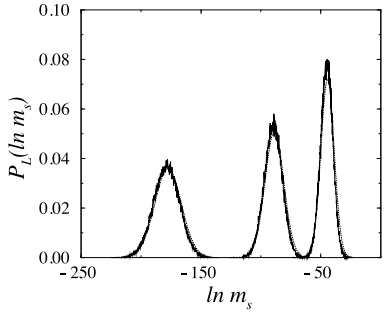

Figure 10. Probability distribution of $\ln m_s$ calculated on 10^5 samples for model #2 with a relevant perturbation. The amplitude is $a_2 = -0.5$ and the decay exponent $\kappa = 0.5$. The chain sizes are $L = 2^{10}$, 2^{12} and 2^{14} from right to left. The dotted curves correspond to the normal distribution in equation (4.2) when the contribution of the dual magnetization to $\ln m_s$ is neglected.

6. Discussion

The two models of extended surface disorder studied in this paper lead to a surface critical behaviour which is quite similar to that obtained in the HvL model, with continuously varying exponents in the marginal case and a stretched exponential behaviour for relevant perturbations. The main differences are the non-self-averaging behaviour of the random models and the log-periodicy obtained with model #2.

This log-periodic behaviour is easily understood if one considers the expression of the surface magnetization in equation (3.8). At criticality $h_l = J = 1$ and, according to (1.3), $\ln J_l$ is either 0 for unperturbed couplings or $\ln(1 + a_2)$ for perturbed ones. A sample α with n_α modified couplings contributes to the probability distribution $P_L(\ln m_s)$ at a value $n_\alpha \ln(1 + a_2) + \ln \overline{m}^{d}_{s\alpha}$ of $\ln m_s$. If the fluctuations of the last term from sample to sample are sufficiently weak compared to the interval $\ln(1 + a_2)$ a modulation with period $\ln(1 + a_2)$ is obtained for $P_L(\ln m_s)$. The argument does not hold for model #1 since the values of the couplings vary from site to site. The absence of modulation for model #2 with a relevant perturbation gives a lower bound for the influence of the disorder on the second surface.

The connection to the HvL model can be clarified through the introduction of effective HvL models describing either the average or the typical behaviour. As long as the size dependence of the dual magnetization in equation (3.8) is the same as for an unperturbed surface, one may introduce effective HvL interactions such that

$$[J_l]^{\rm eff}_{\rm av} = [J_l]_{\rm av} \qquad [J_l]^{\rm eff}_{\rm typ} = \exp([\ln J_l]_{\rm av}). \tag{6.1}$$

Equations (1.2) and (1.3) then lead to:

$$\left.\begin{aligned} [J_l]^{\rm eff}_{\rm av} &= J \\ [J_l]^{\rm eff}_{\rm typ} &\simeq J\left(1 - \tfrac{a_1^2}{2l^{2\kappa}}\right) \end{aligned}\right\} \quad \text{(model \#1)}$$

$$\left.\begin{aligned} [J_l]^{\rm eff}_{\rm av} &= J\left(1 + \tfrac{a_2}{l^{\kappa}}\right) \\ [J_l]^{\rm eff}_{\rm typ} &\simeq J\left[1 + \tfrac{\ln(1+a_2)}{l^{\kappa}}\right] \end{aligned}\right\} \quad \text{(model \#2).} \tag{6.2}$$

For model #1, $\kappa_{\rm HvL} = 2\kappa$ and the random perturbation is marginal at $\kappa_1 = \frac{1}{2}$. The effective amplitude vanishes for averaged quantities whereas it is always negative, with $[a]^{\rm eff}_{\rm typ} = -a_1^2/2$,

for typical quantities. Hence the surface transition is always continuous and the marginal exponents in (4.1) and (4.4) follow from (3.9) with the appropriate effective amplitude.

For model #2, $\kappa_{\mathrm{HvL}} = \kappa$ leads to $\kappa_2 = 1$. The effective amplitudes are $[a]^{\mathrm{eff}}_{\mathrm{av}} = a_2$ and $[a]^{\mathrm{eff}}_{\mathrm{typ}} = \ln(1 + a_2)$. The continuously varying exponent can be deduced from the HvL results when the transition is continuous, in this case even for relevant perturbations (compare (5.1), (5.2) and (3.10)).

One may go further and conjecture the form of the scaling dimension of the surface energy density in the second-order regime. Its value $x^{\mathrm{s}}_{\mathrm{e}} = 2(1 - a)$ for the HvL model [23] translates into:

$$\left.\begin{array}{l} [x^{\mathrm{s}}_{\mathrm{e}}]_{\mathrm{av}} = 2 \\ [x^{\mathrm{s}}_{\mathrm{e}}]_{\mathrm{typ}} = 2 + a_1^2 \end{array}\right\} \quad \text{(model \#1)}$$

$$\left.\begin{array}{ll} [x^{\mathrm{s}}_{\mathrm{e}}]_{\mathrm{av}} = 2(1 - a_2) & a_2 \leqslant 1/2 \\ [x^{\mathrm{s}}_{\mathrm{e}}]_{\mathrm{typ}} = 2[1 - \ln(1 + a_2)] & a_2 \leqslant \sqrt{\mathrm{e}} - 1 \end{array}\right\} \quad \text{(model \#2).} \tag{6.3}$$

As already mentioned, the inhomogeneously disordered Ising quantum chain corresponds to the extreme anisotropic limit of a two-dimensional classical Ising model with correlated disorder along the rows parallel to its surface. It is easy to apply the considerations of section 2 to the case where the perturbations of the different bonds (or sites) at a distance l from the surface of a d-dimensional classical system are independent random variables distributed according to (1.2) or (1.3), i.e., with d-dimensional inhomogeneous disorder.

For model #2, to first order, the perturbation amplitude A_2 transforms like in (2.9) with a scaling dimension $y_\phi - \kappa$ when it couples to the field $\phi(\boldsymbol{r})$ in d dimensions. The off-diagonal second-order correction has the same behaviour. The diagonal second-order correction, with scaling dimension $2y_\phi - \kappa - d$, cannot be more relevant than the first-order correction since $y_\phi \leqslant d$. Thus the relevance of the perturbation remains the same as for the HvL model.

For model #1, however, the scaling dimension of the second-order perturbation amplitude A_1^2 in equation (2.6) changes to $y_{A_1^2} = 2y_\phi - 2\kappa - d$. Thus a thermal perturbation is marginal when $\kappa = 1/\nu - d/2 = \alpha/(2\nu)$ where α is the bulk specific heat exponent. For the two-dimensional Ising model, with $\alpha = 0$, the perturbation is irrelevant as soon as $\kappa > 0$ and marginal for homogeneous disorder, a well-known result [24]. The two-dimensional q-state Potts model would be more interesting since marginal behaviour then corresponds to $\kappa = \frac{1}{5}$ for $q = 3$ ($\nu = \frac{5}{6}$) and $\kappa = \frac{1}{2}$ for $q = 4$ ($\nu = \frac{2}{3}$) [25]. One could then interpolate between a marginal inhomogeneous perturbation and a relevant homogeneous one. Another case of interest is the two-dimensional q-state Potts model with $q > 4$. Here the pure system has a first-order bulk transition [26, 27], the surface transition is continuous [28, 29] and homogeneous disorder changes the bulk transition from first to second order [30–32]. With $\nu = \frac{1}{2}$ at the discontinuity fixed point [33, 34], the critical decay exponent for marginal behaviour is $\kappa = 1$. Varying κ from 1 to 0 could lead to interesting new phenomena.

To conclude, let us mention that it would be useful to adapt Fisher's renormalization group approach to the type of perturbations considered in this work.

Acknowledgments

This work has been supported by the French–Hungarian cooperation programme Balaton (Ministère des Affaires Etrangères-OMFB), the Hungarian National Research Fund under grants No TO23642 and M 028418 and by the Hungarian Ministery of Education under grant No FKFP 0765/1997. The Laboratoire de Physique des Matériaux is Unité Mixte de Recherche CNRS No 7556.

References

[1] Rieger H and Young A P 1997 *Complex Behavior of Glassy Systems (Lecture Notes in Physics vol 492)* ed M Rubi and C Perez-Vicente (Heidelberg: Springer) p 256
[2] Fisher D S 1992 *Phys. Rev. Lett.* **69** 534
[3] Fisher D S 1995 *Phys. Rev.* B **51** 6411
[4] Young A P and Rieger H 1996 *Phys. Rev.* B **53** 8486
[5] Iglói F and Rieger H 1997 *Phys. Rev. Lett.* **78** 2473
[6] Young A P 1997 *Phys. Rev.* B **56** 11 691
[7] Rieger H and Iglói F 1997 *Europhys. Lett.* **39** 135
[8] Iglói F and Rieger H 1998 *Phys. Rev.* B **57** 11 404
[9] Iglói F and Rieger H 1998 *Phys. Rev.* E **58** 4238
[10] Iglói F, Juhász R and Rieger H 1999 *Phys. Rev.* B **59** 11 308
[11] Hilhorst H J and van Leeuwen J M J 1981 *Phys. Rev. Lett.* **47** 1188
[12] Blöte H W J and Hilhorst H J 1983 *Phys. Rev. Lett.* **51** 20
[13] Blöte H W J and Hilhorst H J 1985 *J. Phys. A: Math. Gen.* **18** 3039
[14] Cordery R 1982 *Phys. Rev. Lett.* **48** 215
[15] Burkhardt T W 1982 *Phys. Rev. Lett.* **48** 216
[16] Burkhardt T W 1982 *Phys. Rev.* B **25** 7048
[17] Turban L 1999 *Eur. Phys. J.* B to appear
[18] Kogut J 1979 *Rev. Mod. Phys.* **51** 659
[19] Lieb E H, Schultz T D and Mattis D C 1961 *Ann. Phys., NY* **16** 406
[20] Peschel I 1984 *Phys. Rev.* B **30** 6783
[21] Henkel M and Schütz G 1988 *J. Phys. A: Math. Gen.* **21** 2617
[22] Sornette D 1998 *Phys. Rep.* **297** 239
[23] Iglói F, Peschel I and Turban L 1993 *Adv. Phys.* **42** 683
[24] Harris A B 1974 *J. Phys. C: Solid State Phys.* **7** 1671
[25] Wu F Y 1982 *Rev. Mod. Phys.* **54** 235
[26] Baxter R J 1973 *J. Phys. C: Solid State Phys.* **6** L445
[27] Baxter R J 1982 *J. Phys. A: Math. Gen.* **15** 3329
[28] Lipowsky R 1982 *Phys. Rev. Lett.* **49** 1575
[29] Iglói F and Carlon E 1999 *Phys. Rev.* B **59** 3783
[30] Imry Y and Wortis M 1979 *Phys. Rev.* B **19** 3580
[31] Aizenman M and Wehr J 1989 *Phys. Rev. Lett.* **62** 2503
[32] Hui K and Berker A N 1989 *Phys. Rev. Lett.* **62** 2507
[33] Nienhuis B and Nauenberg M 1975 *Phys. Rev. Lett.* **35** 477
[34] Fisher M E and Berker A N 1982 *Phys. Rev.* B **26** 2507